



NUMERICAL ANALYSIS OF EFFECTIVE PROPERTIES OF INHOMOGENEOUSLY POLARIZED POROUS PIEZOELECTRIC CERAMICS WITH NI-DOPED PORE WALLS CONSIDERING THE INFLUENCE OF VOLUME FRACTIONS OF METAL AND PORES

A.V. Nasedkin¹ and M.E Nassar^{1,2}

¹*Southern Federal University, Rostov-on-don, Russian Federation*

²*Menoufia University, Menouf, Egypt*

The paper considers a porous piezoelectric composite with metal layers deposited on the interface between the piezoelectric and vacuum phases. Such metal layers can be added technologically to improve the mechanical and electromechanical properties of the composite. To find effective modules, we designed a simple representative cubic volume of a unit cell, consisting of a piezoelectric matrix with a compound spherical pore in its center. In turn, the compound pore includes the pore itself and a hollow metal sphere on its surface. The three phases of the composite were modeled as piezoelectric materials. The conducting interface layer was modeled as a piezoelectric material with very high dielectric constants, small piezoelectric moduli, and elastic properties of the employed metal, while the vacuum pore was modeled as a piezoelectric material with marginal moduli. A mathematical formulation of the boundary value problems of homogenization with full contact conditions at the interface boundaries, based on the Hill energy criterion, was described. By solving nine boundary value problems of electroelasticity with different boundary conditions for displacements and electric potential using the finite element method, a complete set of effective moduli of the piezoelectric composite was determined. The importance of considering the inhomogeneous polarization due to the presence of pores and metallic inclusions was discussed. An approximate method was proposed for determining the inhomogeneous polarization field in a piezoceramic matrix, based on a preliminary solution of the electrostatic problem of dielectrics and on locating the elemental coordinate systems rotated along the polarization vector. The paper describes the results of computational experiments for a piezocomposite consisting of PZT-5H piezoceramic matrix, pores, and nickel layers on the pore surfaces. Comparisons between the effective properties of the composite with different volume fractions of metal and a conventional porous piezocomposite were made, depending on the porosity, and taking into account the inhomogeneous polarization. Significant differences were observed of some piezomoduli and dielectric constants, which are promising for various practical applications of the considered composites in piezoactuators operating on the use the phenomenon of the transverse piezoelectric effect.

Key words: piezoelectric composites, porous piezoceramics, piezoelectric ceramic-metal composite, homogenization problem, effective properties, finite element method, piezoelectric transducers, nonuniform polarization

1. Introduction

Due to the unique property of electromechanical coupling, piezoelectric materials are currently used in a wide range of applications, including ultrasonic medical technology, aerospace industry, smart materials technologies, microelectromechanical (MEMS) systems, nondestructive testing, and others [1–5]. Piezoelectric ceramics are the most commonly utilized piezoelectric materials, since they have high piezoelectric moduli, and the technology used to create them makes it possible to control their key properties. Furthermore, by introducing controllable porosity into a piezoelectric material, the efficiency of piezoelectric ultrasonic devices can be significantly enhanced [6, 7]. Porous piezoelectric composites have greater piezoelectric voltage moduli, lower acoustic impedance, and superior hydrostatic properties than dense piezoelectric ceramics [8, 9]. However, piezoceramics and, consequently, porous piezoceramic composites are rather brittle materials, which limits their use [10, 11]. Degradation of the stiffness characteristics of porous piezocomposites at high porosity can result in mechanical damage, dielectric breakdown, and reduced reliability of devices made of these materials [12, 13].

The inclusion of metal particles into a piezoelectric matrix can considerably optimize its mechanical characteristics, particularly, reduce the fracture toughness [14, 15]. To improve the mechanical, electrical, and functional properties of porous piezoceramic composites A.N. Rybyanetset et al. [16, 17] devised a new technique of producing piezocomposites in which polymer microgranules of various forms filled or coated with metal-containing micro- or nanoparticles are introduced into the piezoceramic matrix during the manufacturing process. Therefore, it is feasible to create a porous piezocomposite with metal layers placed at the interfaces between the piezoelectric matrix and vacuum inclusions. In this work, the novel porous piezoceramic composite with metal inclusions and the conventional porous piezocomposite are denoted for brevity as SMPS (a system with metallized pore surfaces) and OPS (an ordinary porous system), respectively. The homogenization problem of SMPS has several features: SMPS is a three-phase composite with closed porosity and, accordingly, with a closed metallization structure, that is, a composite of 3-0-0 connectivity (following R.E. Newnham's terminology [18]).

Despite the presence of the conductive metal inclusions, SMPS is a dielectric medium at the macroscale due to the assumed closed porosity. However, its constitutive relations are quite different. Solving the homogenization problem of SMPS, metal inclusions might be regarded as piezoelectric materials with extremely large dielectric constants and very small piezomoduli, as in the works [19, 20].

Another feature of SMPS is its significant heterogeneity at the microscale level. Although a pure piezoceramic medium is often regarded as a transversely isotropic material uniformly polarized around the Ox_3 axis, this assumption is considerably less justified for SMPS. Indeed, even in OPS, the characteristics of the piezoceramic matrix material near the pores might differ from those of the corresponding dense piezoceramic material. Due to the substantial inhomogeneity enhanced in SMPS, the characteristics of the piezoceramic matrix near the pore walls with metal inclusions become functions of spatial coordinates. In this context, we examine the influence of the inhomogeneity of the polarization field on the effective modules. The inhomogeneity of the polarization vectors in a representative volume of the composite is determined by solving the electrostatics problem, which models the polarization process of piezoelectric ceramics, as described earlier in [19, 21–23]. After that, the homogenization problems of SMPS and OPS can be handled using the recalculated moduli of uniformly polarized piezoceramics considering local coordinate systems with the Ox_3 axes parallel to the directions of the obtained polarization vectors.

The effect of polarization inhomogeneity on the effective properties of SMPS was investigated in [19]. However, the metal layer formed on the pore surface was considered to have a negligible thickness in this study, hence, its elastic characteristics were ignored. As a modification of the approach of [19], the stiffness properties of the metal layer were included in the SMPS model. The effective properties of SMPS and OPS were determined using the effective moduli method and the finite element analysis of the homogenization problems over a simple representative volume element (RVE), as described in [19]. Here, the RVE was regarded as a piezoceramic cube with a spherical pore in the center and a spherical metal layer at the interface between the piezoelectric and vacuum phases. To perform numerical calculations, a collection of algorithms was developed in the ANSYS APDL finite element package. These algorithms implement all steps of homogenization problems for the piezocomposites under consideration.

As a result of these numerical experiments, considering the inhomogeneity of the polarization field, the effective modules were shown to be dependent on the volume fraction of porosity and the portion of metal inclusions. When the inhomogeneity of the polarization field was taken into account, the piezoelectric coefficients fluctuated more than the other coefficients. In addition, the thickness of the metal layer has a significant impact on the effective piezoelectric modules.

2. Mathematical model

The key components of the formulation of the homogenization problem for the described piezocomposites are the governing equations, conditions at the interphase boundaries, external

boundary conditions, and the structure of the representative volume. As in [19, 20, 22, 24], the equations are formulated in the framework of the linear theory of electroelasticity, and the boundary conditions were selected in accordance with the theory of effective modules.

2.1. Representative volume element (RVE)

In order to show the key characteristics of the studied types of piezocomposites, we will consider a simple RVE (unit cell) model. The RVE of SMPS was modeled as a cube Ω inside which a compound spherical pore Ω_p (the cube and sphere have the same centers), and the remainder of the cube Ω_{pz} filled with the primary piezoelectric material, that is $\Omega = \Omega_{pz} \cup \Omega_p$. The compound pore Ω_p , on the other hand, is made up of a vacuum pore Ω_v and a hollow metal ball Ω_m placed to its boundary: $\Omega_p = \Omega_v \cup \Omega_m$. Assume that the length of the edge of the cube is L , and the maximum radius of a composite spherical pore is $R = L\sqrt[3]{3v_p/(4\pi)}$, where $v_p = |\Omega_p|/|\Omega|$ is the volume fraction of the compound pore. Since the inequality $R < L/2$ must be fulfilled, there is a rather strict constraint on porosity in this model: $v_p < 0,52$. If the metal layer thickness is denoted by h , the radius of the vacuum pore Ω_v will be equal to $R-h$, and the inner and outer radii of the hollow sphere Ω_m are respectively $R-h$ and R . The volume of a metal hollow ball can be calculated by the formula $|\Omega_m| = (4\pi/3)(R^3 - (R-h)^3) = v_m|\Omega_p|$, where $v_m = |\Omega_m|/|\Omega_p|$ is the volume fraction of the metal layer Ω_m in the compound pore Ω_p . For the OPS, the unit cell is simplified, since the layer Ω_m is absent and $\Omega^p = \Omega^v$.

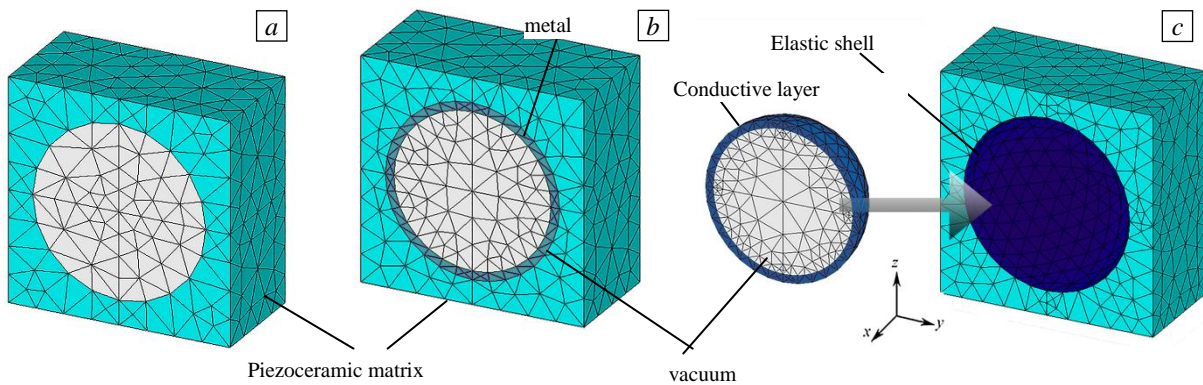


Fig. 1. Half of RVEs for OPS (a), SMPS ($v_m = 0,27$) (b) and SMPS ($v_m = 0,01, h, v_m \rightarrow 0$) (c) at $v_p = 0,25$; – Piezo ceramic matrix, – vacuum, – metal, – Conductive layer, – Elastic shell.

Figures 1a and 1b illustrate instances of OPS and SMPS unit cells sectioned by a plane passing through the center of the pore. They also demonstrate variants of finite element meshes used in different phases of the composite, constructed using ANSYS. The pore is filled with a fictional piezoelectric material with a vacuum dielectric constant and weak piezoelectric and elastic properties. The metal layer is also considered to be a piezoelectric material with nickel elastic characteristics, negligible piezoelectric properties, and a very high dielectric constant.

In Figure 1b, the thickness of the metal layer is $h = R/10$ when $v_m = 0,27$. The use of a RVE similar to that illustrated in Figure 1b is not recommended if the thickness of the metal layer in the SMPS is considerably tiny ($h, v_m \rightarrow 0$), since the small dimensions of the elements in the layer will result in a high number of nodes in the finite element meshes. In this case, the RVE for SMPS (Fig. 1c) is built in a different method, i.e., the metal layer is described as an electrically highly conductive layer surrounded by an elastic shell. The finite shell elements SHELL281 have elastic properties of the metal and the required thickness h . Volumetric finite elements model the electrical

conductivity of a metal layer as a piezoelectric material with a very high dielectric constant and low piezoelectric and elastic properties. As mentioned in [19, 20], the thickness of such a layer that completely covers the pore boundary is negligible; hence, the suggested technique allows one to investigate metal layers with small thicknesses considering their elastic properties. The finite element model shown in Fig. 1c is mainly used to simulate SMPS with a small metal layer thickness. For SMPS with an average thickness of the metal layer ($v_m \leq 0,27$), the obtained effective moduli using both methods of creating the RVE, presented in Figs. 1b and 1c, turn out to be approximately the same.

The finite element models were mainly built using 10 nodal tetrahedral SOLID227 elements with piezoelectric analysis options. The free mesh method from the ANSYS software was used to generate the finite element meshes, with the possibility of setting the maximum length of the element edge. The calculation results were reasonable when the maximum length of the element edge was limited to $L/8$, $L/10$ and $L/16$ for the OPS, the SMPS with $v_m = 0,01$, and SMPS with $v_m = 0,27$, respectively.

2.2. Boundary value homogenization problems

To find the effective moduli of the composites under study, the following boundary value problems of averaging over the volume Ω were solved [19, 20, 22–24]:

$$\mathbf{L}^*(\nabla) \cdot \mathbf{T} = 0, \quad \nabla \cdot \mathbf{D} = 0, \tag{1}$$

$$\mathbf{T} = \mathbf{c}^E \cdot \mathbf{S} - \mathbf{e}^* \cdot \mathbf{E}, \quad \mathbf{D} = \mathbf{e} \cdot \mathbf{S} + \boldsymbol{\varepsilon}^S \cdot \mathbf{E}, \tag{2}$$

$$\mathbf{S} = \mathbf{L}(\nabla) \cdot \mathbf{u}, \quad \mathbf{E} = -\nabla \varphi, \tag{3}$$

$$\mathbf{u} = \mathbf{L}^*(\mathbf{x}) \cdot \mathbf{S}_0, \quad \varphi = -\mathbf{x} \cdot \mathbf{E}_0, \quad \mathbf{x} \in \Gamma = \partial\Omega, \tag{4}$$

$$\mathbf{L}(\nabla) = \begin{bmatrix} \partial_1 & 0 & 0 \\ 0 & \partial_2 & 0 \\ 0 & 0 & \partial_3 \\ 0 & \partial_3 & \partial_2 \\ \partial_3 & 0 & \partial_1 \\ \partial_2 & \partial_1 & 0 \end{bmatrix}, \quad \mathbf{T} = \begin{bmatrix} \sigma_{11} \\ \sigma_{22} \\ \sigma_{33} \\ \sigma_{23} \\ \sigma_{13} \\ \sigma_{12} \end{bmatrix}, \quad \mathbf{S} = \begin{bmatrix} \varepsilon_{11} \\ \varepsilon_{22} \\ \varepsilon_{33} \\ 2\varepsilon_{23} \\ 2\varepsilon_{13} \\ 2\varepsilon_{12} \end{bmatrix}, \quad \nabla = \begin{Bmatrix} \partial_1 \\ \partial_2 \\ \partial_3 \end{Bmatrix}. \tag{5}$$

In expressions (1)–(5) it is accepted: ∇ - nabla operator; σ_{ij} - stress tensor components (hereinafter $i, j = 1, 2, 3$); ε_{ij} — strain tensor components; \mathbf{D} is the vector of electrical induction; \mathbf{E} is the vector of the electric field strength; \mathbf{c}^E — (6×6) matrix of elastic stiffnesses $c_{\alpha\beta}^E$, measured at a constant electric field (hereinafter $\alpha, \beta = 1, 2, \dots, 6$); \mathbf{e} — (3×6) matrix of piezoelectric modules $e_{j\alpha}$; $\boldsymbol{\varepsilon}^S$ - (3×3) matrix of dielectric constants ε_{ii}^S measured at constant deformation; \mathbf{u} - displacement vector; φ - electric potential; $\mathbf{L}(\mathbf{a})$ is a matrix operator depending on the vector $\mathbf{a} = \{a_1, a_2, a_3\}$, which may also be a nabla operator; \mathbf{S}_0 — 6-dimensional array of constant values $S_{0\beta}$; \mathbf{E}_0 — vector of constant values E_{0j} ; $\mathbf{x} = \{x_1, x_2, x_3\} = \{x, y, z\}$ - vector of spatial coordinates; the symbol «*» denotes the operation of transposition, and $(\dots) \cdot (\dots)$ — the dot product. Boundary conditions (4) are typical for the effective moduli theory, but additional clarification is required.

As usual for composite materials, it was assumed that the conditions of full continuity between any two adjacent phases at the interphase boundaries $\Gamma_i = \Gamma_v \cup \Gamma_m$ are fulfilled:

$$[\mathbf{u}] = 0, \mathbf{L}^*(\mathbf{n}) \cdot [\mathbf{T}] = 0, \mathbf{x} \in \Gamma_i \quad (6)$$

$$[\varphi] = 0, \mathbf{n} \cdot [\mathbf{D}] = 0, \mathbf{x} \in \Gamma_i, \quad (7)$$

where the boundaries of a spherical vacuum pore and a hollow metal ball are $\Gamma_v = \partial\Omega_v$ and $\Gamma_m = \partial\Omega_m$, respectively, and $[(...)]$ represents a jump in the value (...) upon passing over the phase boundary.

2.3. Modeling the non-uniform polarization field

The polarization process of a piezoceramic sample can be accomplished by applying a strong electric field that is greater than the coercive field. For carrying out this operation, electrodes are usually applied to the ends of the sample, perpendicular to one of the directions. The dipoles in a polarized piezoceramic sample will thus be mostly oriented in this direction. In general, it is presumed that pure piezoceramics are uniformly polarized in the Ox_3 direction. Meanwhile, porous piezoceramic composites are inhomogeneous at the microscale, therefore, the dipoles and polarization vectors around the pores are not parallel to the main direction of the polarization field. The inhomogeneity of the polarization field influences the effective characteristics of piezoceramic OPS composites, but not considerably when compared to SMPS, as demonstrated in [19]. Indeed, SMPS has metal coatings on the surfaces of the pores, which are electrically conductive and induce a significant polarization field inhomogeneity.

The inhomogeneous polarization will be estimated using a finite element solution of the related electrostatics problem over the RVE of OPS and SMPS, as described in [19, 22–24]. For a cubic volume Ω , such a problem can be formulated as follows

$$\nabla \cdot \mathbf{D} = 0, \mathbf{D} = \varepsilon \mathbf{E}, \mathbf{E} = -\nabla \varphi, \mathbf{x} \in \Omega, \quad (8)$$

$$\varphi = -E_c/L, \mathbf{x} \in \Gamma_{\varphi_1}, \varphi = 0, \mathbf{x} \in \Gamma_{\varphi_2}, \quad (9)$$

$$\mathbf{n} \cdot \mathbf{D} = 0, \mathbf{x} \in \Gamma_q, \quad (10)$$

where $\Gamma = \Gamma_{\varphi_1} \cup \Gamma_{\varphi_2} \cup \Gamma_q$, Γ_{φ_1} and Γ_{φ_2} are the electroded surfaces at $x_3 = -L/2$ and $x_3 = L/2$, E_c — is the value of the polarization field strength, Γ_q — exterior surfaces of the RVE without electrodes, $\varepsilon = \varepsilon(\mathbf{x})$ — piecewise constant dielectric permittivity function (at $\mathbf{x} \in \Omega_{pz}$, $\varepsilon = (2\varepsilon_{11}^s + \varepsilon_{33}^s)/3$); in a metal layer $\mathbf{x} \in \Omega_m$; ε is extremely significant; at the pore $\mathbf{x} \in \Omega_v$, $\varepsilon = \varepsilon_0$; in vacuum $\varepsilon_0 = 8,85 \cdot 10^{-12}$). For the problems (8) – (10), it is also necessary to add interface electrical boundary conditions (7).

The finite element technique is used to solve problems (7) - (10) on a mesh with the same geometry as the subsequent homogenization problems (1) - (7), but with finite elements SOLID227 and the option of solving an electrostatic problem. Using the solution to this problem, the vectors of electric induction \mathbf{D}^{ek} and electric field strength \mathbf{E}^{ek} are obtained at the center point of each finite element Ω^{ek} with number k in the volume of the piezoceramic matrix Ω_{pz} . Consequently, the elemental polarization vectors \mathbf{P}^{ek} may be calculated using the formula:

$$\mathbf{P}^{ek} = \mathbf{D}^{ek} - \varepsilon_0 \mathbf{E}^{ek}. \quad (11)$$

Since the dielectric constants of the piezoelectric phase are substantially greater than the dielectric constant of vacuum, the polarization vectors \mathbf{P}^{ek} will almost coincide with the vectors of electric induction \mathbf{D}^{ek} , according to the second formula from (8) and taking into consideration (11).

Figure 2 illustrates the distributions of vectors \mathbf{D}^{ek} for OPS (Fig. 2a) and SMPS with $v_m = 0,01$ (Fig. 2b). The inhomogeneity of the polarization vector in SMPS is significantly higher than in the OPS, as can be observed from the comparison between Figs. 1a and 1b. This is due to the presence of an electrically conductive layer Ω_m in SMPS. Note that the directions of the polarization vectors in the SMPS with different layer thicknesses Ω_m , for example, at $v_m = 0,01$ and $v_m = 0,27$, are practically the same, since the thickness h of the conducting layer does not affect the solution of the electrostatic problem.

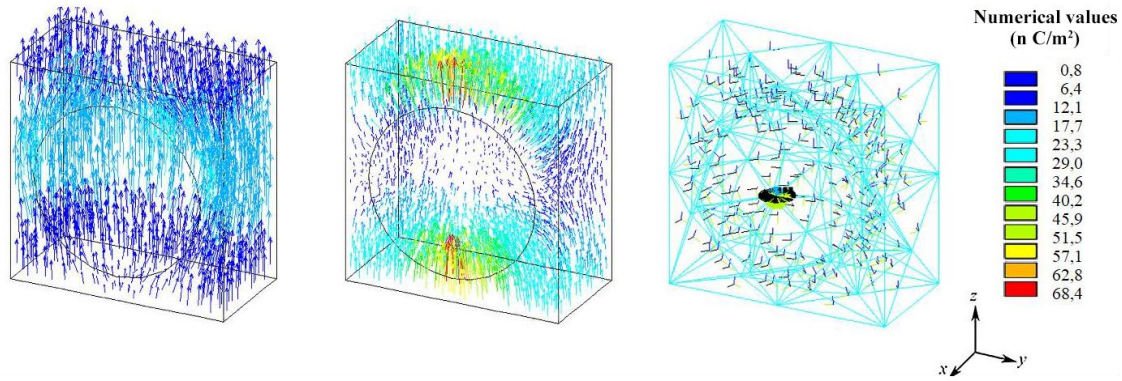


Fig. 2. Vectors of electric induction \mathbf{D}^{ek} at $v_p = 0,25$ for OPS (a), SMPS at $v_m = 0,01$, $v_p = 0,25$ (b); and elemental coordinate systems for the SMPS at $v_m = 0,01$, $v_p = 0,25$ (c)

Then a local (elemental) coordinate system $Ox_1^{ek} x_2^{ek} x_3^{ek}$ is generated for each finite element Ω^{ek} , in which the axis Ox_3^{ek} aligns with the direction of the polarization vector \mathbf{P}^{ek} . If the Ox_3^{ek} axis is not parallel to the Ox_3 axis of the global Cartesian coordinate system, then the Ox_1^{ek} axis is determined by the line of intersection of the plane perpendicular to the Ox_3^{ek} axis and the $Ox_1 x_2$ plane. Then, the direction of the Ox_2^{ek} axis may be easily determined as a line perpendicular to the Ox_3^{ek} and Ox_1^{ek} axes. Only the position of the Ox_3^{ek} axis is important in piezoelectric ceramics, which is a transversely isotropic material at each material point, and the Ox_1^{ek} and Ox_2^{ek} axes can be oriented arbitrarily in the plane perpendicular to Ox_3^{ek} .

The elemental coordinate systems constructed according to the described algorithm are shown in Fig.2c for SMPS with $v_m = 0,01$. For clarity, we used a coarse finite element mesh, whose maximum length of element edges is $L/2$, as seen in Fig. 2c. In reality, fine meshes were used in the calculations for electrostatics problems (7) - (10) and for homogenization problems (1) - (7). Then, problems (1) - (7) were solved taking into account the inhomogeneous polarization as follows: the dielectric elements SOLID227 are replaced by piezoelectric ones with their material properties in accordance with the properties of the phases of the piezoelectric composite, and for each finite element its own elemental coordinate system is determined, which coincides with the local coordinate system $Ox_1^{ek} x_2^{ek} x_3^{ek}$ created at the previous step. According to this technique, the inhomogeneity of the polarization in piezoceramics is only taken into account by recalculating the modules $c_{\alpha\beta}^E$, $e_{j\alpha}$, and ε_{ii}^S , which were originally defined in the global Cartesian coordinate system, into the equivalent moduli in the elemental coordinate systems. This type of recalculation is done automatically in the ANSYS finite element software.

2.4. Effective moduli method for piezoelectric composites

To determine the values of the effective moduli of piezoceramic composites for OPS and SMPS, the technology defined in [19, 20] was implemented, which includes the solution of boundary value problems of electroelasticity (1) - (7) with various non-zero values in boundary conditions (4). So, problems (1) - (7) are solved nine times: six times for one nonzero value S_0 , when equalities are recognized in (4): $S_{0\beta} = S_0\delta_{\beta\zeta}$, $\zeta = 1, 2, \dots, 6$, $E_{0j} = 0$, and three times for one nonzero value of E_0 , that is, for $S_{0\beta} = 0$, $E_{0j} = E_0\delta_{jk}$, $k = \zeta - 6$, $\zeta = 7, 8, 9$. After obtaining solutions $(u_1)_\zeta$, $(u_2)_\zeta$, $(u_3)_\zeta$, $(\varphi)_\zeta$, for each of the problems (1) - (7) with $\zeta = 1, 2, \dots, 9$ the components stress tensor $(T_1)_\zeta = (\sigma_{11})_\zeta$, $(T_2)_\zeta = (\sigma_{22})_\zeta$, $(T_3)_\zeta = (\sigma_{33})_\zeta$, $(T_4)_\zeta = (\sigma_{23})_\zeta$, $(T_5)_\zeta = (\sigma_{13})_\zeta$, $(T_6)_\zeta = (\sigma_{12})_\zeta$ and components of the electric induction vector $(D_i)_\zeta$ were determined in the volume Ω . The integral values of these quantities can also be obtained using the formula:

$$\langle \langle \dots \rangle \rangle = \frac{1}{|\Omega|} \int_{\Omega} (\dots) d\Omega. \tag{12}$$

As a consequence, using the averaged voltages and electrical induction (12), the complete set of effective modules $c_{\alpha\beta}^{E\text{eff}}$, $e_{i\beta}^{\text{eff}}$, and $\varepsilon_{ij}^{S\text{eff}}$ of a piezoelectric composite material may be determined. So, from the solutions of problems (1)–(7) for various nonzero boundary conditions for displacements, when in (4) for a fixed index $\zeta = 1, 2, \dots, 6$, the following equalities are accepted:

$$S_{0\beta} = S_0\delta_{\beta\zeta}, E_{0j} = 0, \tag{13}$$

the effective stiffness moduli $c_{\alpha\zeta}^{E\text{eff}}$ and the effective piezomoduli $e_{i\zeta}^{\text{eff}}$ can be obtained by the following formulas:

$$c_{\alpha\zeta}^{E\text{eff}} = \langle \langle (T_\alpha)_\zeta \rangle \rangle / S_0, e_{i\zeta}^{\text{eff}} = \langle \langle (D_i)_\zeta \rangle \rangle / S_0, \tag{14}$$

where $\alpha = 1, 2, \dots, 6$, $i = 1, 2, 3$.

When solving problems (1) - (7) with various nonzero electrical impacts, the following criteria are satisfied in (4) for $\zeta = 7, 8, 9$, $k = \zeta - 6$, that is, for $k = 1, 2, 3$:

$$S_{0\beta} = 0, E_{0j} = E_0\delta_{jk}, \tag{15}$$

the effective piezomoduli $e_{k\alpha}^{\text{eff}}$ and the effective dielectric constants $\varepsilon_{ik}^{S\text{eff}}$ can be calculated again according to the expressions:

$$e_{k\alpha}^{\text{eff}} = -\langle \langle (T_\alpha)_\zeta \rangle \rangle / E_0, \varepsilon_{ik}^{S\text{eff}} = \langle \langle (D_i)_\zeta \rangle \rangle / E_0. \tag{16}$$

The proposed approach for calculating the effective properties is substantiated in [20, 24]. It can also be applied to piezoelectric composites with inhomogeneous polarization of the piezoceramic matrix, as well as composites with conductive inclusions. Based on limit transitions in analytical solutions of homogenization problems, the method utilized here was validated in [25, 26] for the porous dielectric composites with metalized pore surfaces.

This homogenization method is based on the energy relationships between the heterogeneous composite and the homogenized one, which is known as the Hill relationships for the averaged values in piezoelectric composites [20, 24, 27]:

$$\langle \mathbf{T} \cdot \mathbf{S} \rangle = \langle \mathbf{T} \rangle \cdot \langle \mathbf{S} \rangle, \quad \langle \mathbf{D} \cdot \mathbf{E} \rangle = \langle \mathbf{D} \rangle \cdot \langle \mathbf{E} \rangle, \quad \langle \mathbf{S} \rangle = \mathbf{S}_0, \quad \langle \mathbf{D} \rangle = \mathbf{D}_0. \quad (17)$$

Naturally, homogenization problems (1) - (7) with (12) - (16) can also be solved without taking into account the inhomogeneity of the polarization field. In this simpler case, the piezoceramic matrix is assumed to be an ordinary piezoelectric material of the crystallographic class of 6mm, uniformly polarized along the Ox_3 axis.

When determining the full set of equivalent material properties, we checked the type of anisotropy of the resulting homogeneous material and found that it retains the symmetry class δmm of the piezoceramic matrix except for a small difference between the modulus $c_{66}^{E\text{eff}}$ and $(c_{11}^{E\text{eff}} - c_{12}^{E\text{eff}})/2$. The piezocomposite's principal moduli are therefore ten effective modules: $c_{11}^{E\text{eff}}$, $c_{12}^{E\text{eff}}$, $c_{13}^{E\text{eff}}$, $c_{33}^{E\text{eff}}$, $c_{44}^{E\text{eff}}$, e_{31}^{eff} , e_{33}^{eff} , e_{15}^{eff} , $\varepsilon_{11}^{S\text{eff}}$, and $\varepsilon_{33}^{S\text{eff}}$. However, for the RVEs with strong geometric asymmetry, this kind of anisotropy may be changed.

3. Numerical results

For a composite containing a PZT-5H piezoceramic matrix, nickel inclusions, and vacuum pores, the computational experiments were conducted. In these computations, the following material properties were used for the piezoceramic PZT-5H: $c_{11}^E = 12,6 \cdot 10^{10}$ N/m², $c_{12}^E = 7,95 \cdot 10^{10}$ N/m², $c_{13}^E = 8,41 \cdot 10^{10}$ N/m², $c_{33}^E = 11,7 \cdot 10^{10}$ N/m², $c_{44}^E = 2,3 \cdot 10^{10}$ N/m², $e_{31} = -6,5$ C/m², $e_{33} = 23,3$ C/m², $e_{15} = 17$ C/m², $\varepsilon_{11}^S = 1700\varepsilon_0$, $\varepsilon_{33}^S = 1470\varepsilon_0$.

The vacuum pore was modeled as a piezoelectric material with negligible moduli: $(c_{\alpha\beta}^E)_v = \eta c_{\alpha\beta}^E$, $(e_{i\alpha})_v = \eta$ C/m², $\eta = 10^{-10}$, $(\varepsilon_{ii}^S)_v = \varepsilon_0$. Metal (nickel) was assumed to be a piezoelectric material with negligible piezoelectric moduli: $(e_{i\alpha})_m = \eta$ C/m², and extremely high dielectric permittivity moduli: $(\varepsilon_{ii}^S)_m = \chi\varepsilon_0$, $\chi \gg 1$. Using preliminary studies for the SMPS, the values of the effective moduli became stable already at $\chi = 10^8$. However, the factor χ , for greater reliability regarding all variants of the SMPS was assumed to be 10^{12} .

Nickel was characterized as an isotropic material with a Young's modulus of $E_m = 20,5 \cdot 10^{10}$ N/m² and a Poisson's ratio of $\mu_m = 0,31$. The nickel was chosen as an inclusion of the composite due to its high mechanical rigidity and relatively low cost [28, 29]. Thus, for the material under study, the longitudinal elastic stiffness of nickel was about 225% of the greatest modulus of elasticity c_{11}^E of the PZT-5H piezoceramic.

Due to the insignificant moduli of the hypothetical pore material in the volume Ω_v , the integral values of stresses \mathbf{T} and electric inductions \mathbf{D} in this volume are negligible and have no influence on the values of the effective moduli (14) and (16). As a result, the finite elements in the volume Ω_v could not be included in the RVE. To ensure the correctness of the calculations, the integral characteristics were calculated in all phases of the composite in the APDL ANSYS programs, and the fulfillment of Hill's relations (17), which are valid for various versions of OPS and SMP composites, was checked considering the mechanical and electric fields in the pore and the metal layer.

The following figures show the effective properties of OPS and SMPS composites compared to the corresponding properties of the dense piezoceramic matrix. The equivalent moduli are presented relatively to the analogous moduli of the implemented piezoceramic matrix, for example, are calculated as $r(c_{\alpha\beta}^E) = c_{\alpha\beta}^{E\text{eff}} / c_{\alpha\beta}^E$. In Figs. 3-5, the curves for OPS, SMPS with $v_m = 0,01$, and SMPS with $v_m = 0,27$ are marked with numbers 1, 2, and 3, respectively. In addition, the solid lines show the effective properties of the studied composites with a uniformly polarized piezoceramic matrix;

whereas, the dotted lines show the effective properties taking the inhomogeneity of the polarization field into account.

Figures 3a and 3b show the dependences of the relative effective moduli of rigidity $r(c_{33}^E)$ and $r(c_{13}^E)$, respectively, on the volume fraction of porosity v_p . As can be observed, they decrease monotonically as porosity increases, which is reasonable considering that the elastic moduli of the fictional pore material are insignificant. The effective elastic moduli of the SMPS can be enhanced compared to OPS by increasing the proportion of metal. For example, at $v_p = 0,25$ and $v_m = 0,27$, the elastic moduli $r(c_{33}^E)$ and $r(c_{13}^E)$ for the SMPS increase by 42% and 41.7%, respectively, compared to the same moduli of OPS. The inhomogeneity of the polarization field insignificantly affects the moduli of elastic stiffness. Thus, for $v_p = 0,25$, taking into account the polarization field inhomogeneity, the relative modulus of elasticity $r(c_{33}^E)$ of OPS decreases by 4.06%, but increases by 5.5% and 4.08%, respectively, for SMPS with $v_m = 0,01$ and for SMPS with $v_m = 0,27$ in comparison with a uniformly polarized analogous composites. It is interesting to note that, despite having a metal layer that is more rigid than the piezoceramic matrix, SMPS's (at $v_m = 0,01$) effective elastic stiffness modulus $r(c_{13}^E)$ are smaller than similar OPS modulus. This unusual effect is due to the different values of the piezoelectric contribution to the equivalent elastic moduli of OPS and SMPS.

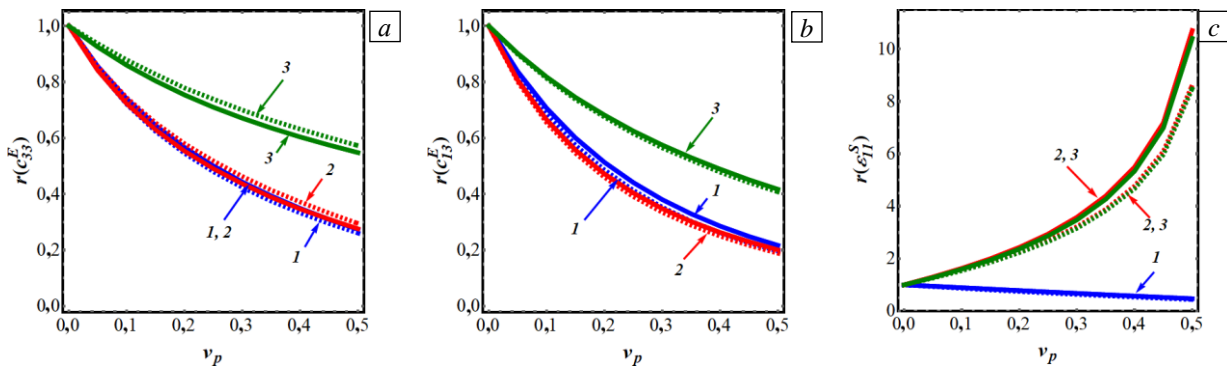


Fig. 3. The relative effective stiffness moduli $r(c_{33}^E)$ (a), $r(c_{13}^E)$ (b), and relative dielectric modulus $r(\epsilon_{11}^S)$ (c) as functions of the porosity volume fraction v_p ; OPS (curve 1), SMPS with $v_m = 0,01$ (2), SMPS with $v_m = 0,27$ (3); homogeneous polarization (solid lines) and inhomogeneous polarization (dotted lines).

Figure 3c depicts the variation in the relative effective dielectric constant $r(\epsilon_{11}^S)$ with porosity. In contrast to the OPS, the relative dielectric permittivity constant $r(\epsilon_{11}^S)$ of SMPS monotonically increases with increasing porosity. Similar results were obtained by the Maxwell formula [26, 27] for conventional dielectric composites with metal inclusions. In SMPS, as in dielectrics with conductive inclusions, the metalized pore surface prevents the propagation of the electric field into the region Ω_p . Therefore, the electric field caused by the electric impact (15) is completely preserved in the region Ω_{pz} occupied by piezoceramics. Its integral value by volume Ω_{pz} is higher than the corresponding integral value in OPS under similar conditions. The effect of metallization of pore surfaces is even more noticeable in the integral value of the electric induction field. As a result, for SMPS, the effective permittivity coefficients determined by (16) increase with the porosity increase, that is, with an increase in the area of metalized surfaces. The discrepancies between the effective dielectric constants of SMPS and OPS become more substantial when the

porosity is large. For example, the relative dielectric permittivity coefficient $r(\epsilon_{11}^S)$ of SMPS at $v_p = 0,4$ increases by 853% compared to the analogous module of the OPS.

Upon increasing porosity, the relative permittivities $r(\epsilon_{11}^S)$ and $r(\epsilon_{33}^S)$ change in approximately the same way. When polarization inhomogeneity is included, the relative dielectric modulus $r(\epsilon_{11}^S)$ decreases for all composite systems, as shown in Fig.3c; at $v_p = 0,25$, the relative dielectric modulus $r(\epsilon_{11}^S)$ of the OPS, SMPS with $v_m = 0,01$, and SMPS with $v_m = 0,27$ decreases by 5.48, 8.5, and 7.67%, respectively. However, the inhomogeneous polarization affects the effective dielectric modulus $r(\epsilon_{33}^S)$ for SMPS to a lesser extent.

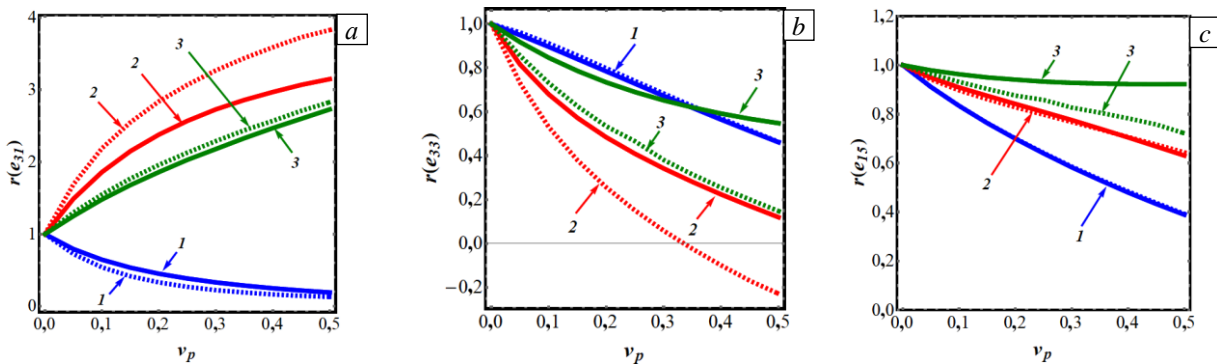


Fig.4. The relative piezoelectric moduli $r(e_{31})$ (a), $r(e_{33})$ (b), and $r(e_{15})$ (c) as functions of the porosity volume fraction v_p ; OPS (curve 1), SMPS with $v_m = 0,01$ (2), SMPS with $v_m = 0,27$ (3); homogeneous polarization (solid lines) and inhomogeneous polarization (dotted lines).

The dependences of piezomoduli $r(e_{31})$, $r(e_{33})$, and $r(e_{15})$ on porosity are shown in Fig. 4. Since the equivalent piezomoduli of the vacuum phase are insignificant, the relative piezomoduli $r(e_{31})$, $r(e_{33})$, and $r(e_{15})$ of OPS decrease with rising porosity. Meanwhile, as shown in Fig.4a, as porosity increases, for SMPS the relative piezoelectric modulus $r(e_{31})$ grows monotonically, but the piezoelectric moduli $r(e_{33})$ and $r(e_{15})$ decrease monotonically. On the contrary, if the volume fraction of the compound pore in SMPS remains constant, and the fraction of metal v_m increases, then this causes a decrease in $r(e_{31})$ and an increase in $r(e_{33})$ and $r(e_{15})$, as seen in Figs. 4b and 4c. The differences between SMPS and OPS piezomoduli can be rather significant, especially the relative modulus $r(e_{31})$. So, at $v_p = 0,3$, the relative piezoelectric coefficient $r(e_{31})$ of the SMPS increases by 726%, and the relative piezomodulus $r(e_{33})$ of the SMPS decreases by 49% compared to the corresponding moduli of the OPS with the same porosity.

Considering the inhomogeneity of the polarization field significantly affects the relative piezomodulus $r(e_{33})$ of the SMPS and the piezomodulus $r(e_{31})$ of SMPS ($v_m = 0,01$), but slightly affects the piezoelectric moduli of OPS, the piezomodulus $r(e_{15})$ of SMPS with $v_m = 0,01$, and the piezomodulus $r(e_{31})$ of SMPS with $v_m = 0,27$ (see Fig. 4). For example, for OPS at $v_p = 0,25$ and taking the non-uniformly polarized field into account, the piezoelectric modulus $r(e_{31})$ decreases by 30.11%, and the piezoelectric modules $r(e_{33})$ and $r(e_{15})$ increase respectively by 1.64% and 0.34% compared to the corresponding OPS moduli with a uniformly polarized piezoceramic matrix. The influence of considering the inhomogeneous polarization field on the piezomoduli $r(e_{31})$ and

$r(e_{33})$ reduces as the amount of metal inclusion increases in SMPS, while its effect on the effective piezomodulus $r(e_{15})$ increases. So, in the SMPS with $v_p = 0,25$, taking the inhomogeneity of the polarization field into account, the relative piezoelectric modulus $r(e_{33})$ decreases by 63.1% and 32.5% from its analogous values for the SMPS with a piezoceramic matrix at $v_m = 0,01$ and $v_m = 0,27$, respectively.

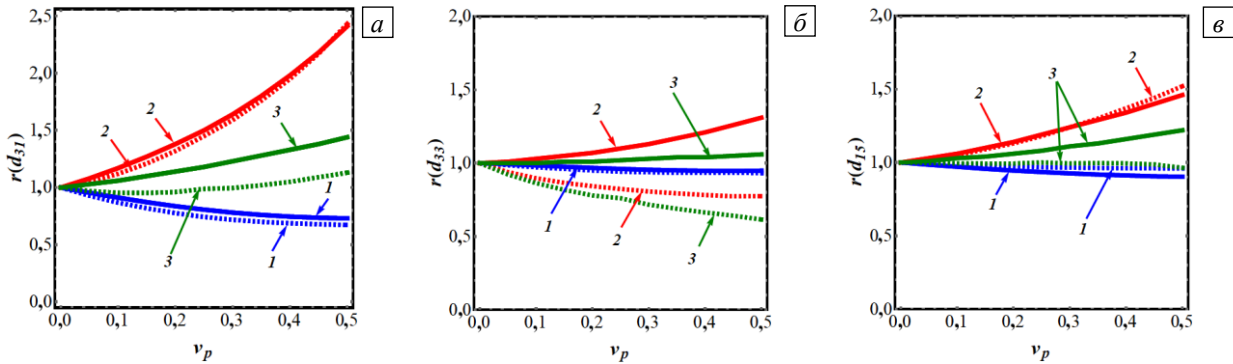


Fig.5. The relative piezoelectric moduli $r(d_{31})$ (a), $r(d_{33})$ (b), and $r(d_{15})$ (c) as functions of the porosity volume fraction v_p ; OPS (curve 1), SMPS with $v_m = 0,01$ (2), SMPS with $v_m = 0,27$ (3); homogeneous polarization (solid lines) and inhomogeneous polarization (dotted lines).

Figure 5 shows the dependencies of the relative piezoelectric strain coefficients $r(d_{31})$, $r(d_{33})$, and $r(d_{15})$ on porosity volume fraction v_p . These piezoelectric moduli are important indicators for evaluating the efficiency of piezoelectric transducers in various practical applications and are determined by the formulas $\mathbf{d}^{\text{eff}} = \mathbf{e}^{\text{eff}} \cdot (\mathbf{c}^{E\text{eff}})^{-1}$. For OPS, the relative piezoelectric moduli $r(d_{31})$ decreases with increasing the volume fraction of porosity v_p , while the values of $r(d_{33})$ and $r(d_{15})$ remain almost constant. However, for the SMPS with a uniform polarization of the piezoceramic matrix, the relative piezoelectric strain coefficients increase monotonically with the porosity rise, especially the coefficient $r(d_{31})$. As can be seen in Fig. 5, the relative piezomoduli $r(d_{31})$, $r(d_{33})$, and $r(d_{15})$ of the SMPS decrease with the increase the metal volume fraction. Taking the inhomogeneous polarization into account insignificantly affects the relative piezomoduli $r(d_{31})$, $r(d_{33})$, and $r(d_{15})$ of the OPS, as well as $r(d_{31})$ and $r(d_{15})$ of the SMPS with $v_m = 0,01$. For example, considering the inhomogeneity of the polarization field for the OPS at $v_p = 0,4$, the piezo moduli $r(d_{31})$ and $r(d_{33})$ decrease by 7.8% and 1.4%, respectively; however, the piezomodulus $r(d_{15})$ increases by 5.4% compared to the analogous equivalent moduli for the OPS with uniform polarization. In general, considering the inhomogeneous polarization has a more significant effect on the SMPS's equivalent moduli. The piezoelectric strain coefficients become more dependent on polarization field inhomogeneity as the metal volume percentage increases. So, considering the inhomogeneity of the polarization field at $v_p = 0,3$ and $v_m = 0,27$, the piezoelectric moduli $r(d_{31})$, $r(d_{33})$, and $r(d_{15})$ decrease by 19%, 30,4% and 10,5% compared to corresponding moduli of the same composites with a uniformly polarized piezoceramic matrix.

4. Conclusions

The article looks into the homogenization problem of insufficiently researched porous piezoelectric composite with a metal coating at the pore boundaries. Such a composite, called SMPS, has a number of better mechanical and electromechanical properties compared to an ordinary porous system (OPS). The macro properties of the investigated piezocomposites were analyzed using computer modeling based on the finite element analysis, which considered the porosity and volume fraction of the metal in which the pores are enclosed. The influence of the polarization field inhomogeneity on the equivalent properties of SMPS and OPS has been studied. The presence of metal inclusion in SMPS increases the electric field and polarization at the interface between the piezoelectric and metallic phases, which causes a drastic change in the effective piezoelectric and dielectric permittivity moduli of this system compared to OPS. Considering the non-uniform polarization has a less significant effect on effective moduli of OPS. It was found that the transverse piezomodulus $|d_{31}^{\text{eff}}|$ and the shear piezomodulus d_{15}^{eff} of SMPS turn out to be higher than the OPS, especially for small metal fractions in their volume. This fact allows us to recommend porous piezo composites with metalized pore surfaces as active materials for piezoelectric transducers operating on the use of transverse and shear piezoelectric strain coefficients.

As a continuation of this research, we plan to consider the homogenization problems for more complex representative volumes of SMPS, with partial metal coating of the pore surfaces. We also intend to computationally model the piezoelectric emitters with active elements made of SMPS materials.

Acknowledgement: This research was done in the framework of the RFBR project 20-31-90102.

References

1. Vijaya M.S. *Piezoelectric materials and devices: Applications in engineering and medical sciences*. CRC press, 2012. 186 p. <https://doi.org/10.1201/b12709>
2. Elahi H., Munir K., Eugeni M., Abrar M., Khan A., Arshad A., Gaudenzi P. A review on applications of piezoelectric materials in aerospace industry. *Integrated Ferroelectrics*, 2020, vol. 211, pp. 25-44. <https://doi.org/10.1080/10584587.2020.1803672>
3. Gripp J.A.B., Rade D.A. Vibration and noise control using shunted piezoelectric transducers: A review. *Mech. Syst. Signal Process.*, 2018, vol. 112, pp. 359-383. <https://doi.org/10.1016/j.ymsp.2018.04.041>
4. Wang L.-P., Wolf R.A., Wang Y., Deng K.K., Zou L., Davis R.J., Trolier-McKinstry S. Design, fabrication, and measurement of high-sensitivity piezoelectric microelectromechanical systems accelerometers. *J. Microelectromech. Syst.*, 2003, vol. 12, pp. 433-439. <https://doi.org/10.1109/JMEMS.2003.811749>
5. Brownjohn J.M.W. Structural health monitoring of civil infrastructure. *Phil. Trans. R. Soc. A*, 2007, vol. 365, pp. 589-622. <https://doi.org/10.1098/rsta.2006.1925>
6. Smith W.A. The role of piezocomposites in ultrasonic transducers. *Proc. IEEE Ultrasonics Symp.*, 1989, vol. 2, pp. 755-766. <https://doi.org/10.1109/ULTSYM.1989.67088>
7. Della C.N., Shu D. The performance of 1-3 piezoelectric composites with a porous non-piezoelectric matrix. *Acta Mater.*, 2008, vol. 56, pp. 754-761. <https://doi.org/10.1016/j.actamat.2007.10.022>
8. Iyer S., Venkatesh T.A. Electromechanical response of porous piezoelectric materials: Effects of porosity connectivity. *Appl. Phys. Lett.*, 2010, vol. 97, 072904. <https://doi.org/10.1063/1.3481416>
9. Iyer S., Venkatesh T.A. Electromechanical response of (3-0) porous piezoelectric materials: Effects of porosity shape. *J. Appl. Phys.*, 2011, vol. 110, 034109. <https://doi.org/10.1063/1.3622509>
10. Yoon S.-J., Moon J.H., Kim H.-J. Piezoelectric and mechanical properties of $\text{Pb}(\text{Zr}_{0.52}\text{Ti}_{0.48})\text{O}_3\text{-Pb}(\text{Y}_{2/3}\text{W}_{1/3})\text{O}_3$ (PZT-PYW) ceramics. *J. Mater. Sci.*, 1997, vol. 32, pp. 779-782. <https://doi.org/10.1023/A:1018516608868>
11. Mehta K., Virkar A.V. Fracture mechanisms in ferroelectric-ferroelastic lead zirconate titanate (Zr: Ti=0.54:0.46) ceramics. *J. Am. Ceram. Soc.*, 1990, vol. 73, pp. 567-574. <https://doi.org/10.1111/j.1151-2916.1990.tb06554.x>

12. Liu W., Li N., Wang Y., Xu H., Wang J., Yang J. Preparation and properties of 3–1 type PZT ceramics by a self-organization method. *J. Eur. Ceram. Soc.*, 2015, vol. 35, pp. 3467-3474. <https://doi.org/10.1016/j.jeurceramsoc.2015.06.007>
13. Xiang P.-H., Dong X.-L., Chen H., Zhang Z., Guo J.-K. Mechanical and electrical properties of small amount of oxides reinforced PZT ceramics. *Ceram. Int.*, 2003, vol. 29, pp. 499-503. [https://doi.org/10.1016/S0272-8842\(02\)00193-1](https://doi.org/10.1016/S0272-8842(02)00193-1)
14. Zhang H.L., Li J.-F., Zhang B.-P. Fabrication and evaluation of PZT/Ag composites and functionally graded piezoelectric actuators. *J. Electroceram.*, 2006, vol. 16, pp. 413-417. <https://doi.org/10.1007/s10832-006-9890-4>
15. Takagi K., Li J.-F., Yokoyama S., Watanabe R. Fabrication and evaluation of PZT/Pt piezoelectric composites and functionally graded actuators. *J. Eur. Ceram. Soc.*, 2003, vol. 23, pp. 1577-1583. [https://doi.org/10.1016/S0955-2219\(02\)00407-7](https://doi.org/10.1016/S0955-2219(02)00407-7)
16. Rybyanets A. N., Shvetsov I.A., Lugovaya M.A., Petrova E.I., Shvetsova N.A. Nanoparticles transport using polymeric nano- and microgranules: novel approach for advanced material design and medical applications. *J. Nano- Electron. Phys.*, 2018, vol. 10, 02005. [https://doi.org/10.21272/jnep.10\(2\).02005](https://doi.org/10.21272/jnep.10(2).02005)
17. Rybyanets A.N., Naumenko A.A. Nanoparticles transport in ceramic matrices: A novel approach for ceramic matrix composites fabrication. *J. Mod. Phys.*, 2013, vol. 4, pp. 1041-1049. <https://doi.org/10.4236/jmp.2013.48140>
18. Newnham R.E., Skinner D.P., Cross L.E. Connectivity and piezoelectric-pyroelectric composites. *Mater. Res. Bull.*, 1978, vol. 13, pp. 525-536. [https://doi.org/10.1016/0025-5408\(78\)90161-7](https://doi.org/10.1016/0025-5408(78)90161-7)
19. Nasedkin A., Nassar M.E. Effective properties of a porous inhomogeneously polarized by direction piezoceramic material with full metalized pore boundaries: Finite element analysis. *J. Adv. Dielect.*, 2020, vol. 10, 2050018. <http://doi.org/10.1142/S2010135X20500186>
20. Nasedkin A.V., Nasedkina A.A., Nassar M.E. Homogenization of porous piezocomposites with extreme properties at pore boundaries by effective moduli method. *MechSolids*, 2020, vol. 55, pp. 827-836. <https://doi.org/10.3103/S0025654420050131>
21. Martínez-Ayuso G., Friswell M.I., Khodaparast H.H., Roscow J.I., Bowen C.R. Electric field distribution in porous piezoelectric materials during polarization. *Acta Mater.*, 2019, vol. 173, pp. 332-341. <https://doi.org/10.1016/j.actamat.2019.04.021>
22. Gerasimenko T.E., Kurbatova N.V., Nadolin D.K., Nasedkin A.V., Nasedkina A.A., Oganessian P.A., Skaliukh A.S., Soloviev A.N. Homogenization of piezoelectric composites with internal structure and inhomogeneous polarization in ACELAN-COMPOS finite element package. *Wave dynamics, mechanics and physics of microstructured metamaterials*, ed. M. Sumbatyan. Springer, 2019. Pp. 113-131. https://doi.org/10.1007/978-3-030-17470-5_8
23. Nasedkin A.V., Nasedkina A.A., Rybyanets A.N. Numerical analysis of effective properties of heterogeneously polarized porous piezoceramic materials with local alloying pore surfaces. *Materials Physics & Mechanics*, 2018, vol. 40, no. 1, pp. 12-21. http://dx.doi.org/10.18720/MPM.4012018_3
24. Nasedkin A.V., Shevtsova M.S. Improved finite element approaches for modeling of porous piezocomposite materials with different connectivity. *Ferroelectrics and superconductors: Properties and applications*, ed. I.A. Parinov. New York, Nova Science Publ., 2011. Pp. 231-254.
25. Kudimova A.B., Nasedkin A.V. Limit transitions in plane homogenization problems for two-phase dielectric composites with extreme material properties of one phase. *J. Phys.: Conf. Ser.*, 2021, vol. 1847, 012039. <https://doi.org/10.1088/1742-6596/1847/1/012039>
26. Kudimova A.B., Nasedkin A.V. About limit transitions in spatial homogenization problems for two-component dielectric composites with extremal moduli for one of phases. *Izv. vuzov. Severo-Kavkazskiy region. Estestvennyye nauki – Bulletin of Higher Educational Institutions. North Caucasus Region. Natural Sciences*, 2021, no. 1, pp. 25-32. <https://doi.org/10.18522/1026-2237-2021-1-25-32>
27. Hori M., Nemat-Nasser S. Universal bounds for effective piezoelectric moduli. *Mech. Mater.*, 1998, vol. 30, pp. 1-19. [https://doi.org/10.1016/S0167-6636\(98\)00029-5](https://doi.org/10.1016/S0167-6636(98)00029-5)
28. Wang J., Li W. A new piezoelectric hollow cylindrical transducer with multiple concentric annular metal fillers. *Mater. Res. Express*, 2019, vol. 6, 055701. <https://doi.org/10.1088/2053-1591/ab0318>
29. Du H., Lin X., Zheng H., Qu B., Huang Y., Chu D. Colossal permittivity in percolative ceramic/metal dielectric composites. *Journal of Alloys and Compounds*, 2016, vol. 663, pp. 848-861. <https://doi.org/10.1016/j.jallcom.2015.12.171>

The authors declare no conflict of interests.

The paper was received on 16.04.2021 and accepted for publication on 19.05.2021.